Available online www.jsaer.com

***Journal of Scientific and Engineering Research*, 2023, 10(2):127-133**

Research Article

ISSN: 2394-2630
CODEN(USA): JSERBR

Fluid-structure Interaction Analysis of Double Suction Liquid Ring Pump Impeller

Zhang Yaowen*, Zhang Yuxue, Zhao Xu, Zhao Peidong

* School of Engineering, Transportation and Vehicle Engineering, Shandong University of Technology, Zibo, China. E-mail:zhangyaowen7101@163.com

Abstract By using the ANSYS Workbench simulation software and based on the principle of unidirectional fluid-structure coupling, the stress and strain of the double-suction liquid-ring pump impeller and the rotor mode are analyzed, and the stress and deformation distribution of the impeller under different working conditions and the rotor modes are obtained. The results show that the stress distribution of the impeller of the liquid ring pump is uneven and there is local stress concentration. The impeller deformation increases with the radius, and reaches the maximum at the edge of the impeller. The deformation and equivalent stress distribution on the working face and back of the blade are approximately the same, but the maximum stress on the working face is higher than that on the back. The stiffener effectively alleviates the deformation of the impeller edge. The maximum deformation under different working conditions is 0.14414mm, and the maximum stress is 20.572MPa. The calculation results meet the mechanical performance requirements. The difference between the rotating speed of the liquid ring pump and the critical rotating speed is large, and resonance is not easy to occur.

Keywords fluid-structure interaction, numerical simulation, liquid ring pump, total deformation, modal

Introduction

The impeller is one of the most important parts of the liquid ring pump. The deformation and stress generated by the impeller have an important influence on the stable operation and working life of the liquid ring pump [1]. For the rotating structure, if its natural frequency coincides with or is similar to the excitation frequency generated by the rotation of the system, it will cause resonance of the structure, which will increase the vibration of the structure and lead to accidents [2,3].

The structural analysis of fluid machinery mainly focuses on stress-strain analysis and modal analysis. The research on structural analysis of pump machinery by fluid-solid coupling method has been relatively mature. Li Peijian [4] used fluid-solid coupling method to analyze the stress state of the tangential pump when coupling the flow field pressure. The maximum stress is less affected by the flow field pressure, and the stress of individual blades will increase. Zhang Xin [5] and Zhu Li [6] used ANSYS software to calculate the strength of axial flow pump impeller by one-way fluid-solid coupling, determined the stress concentration area, and obtained the stress distribution law. The results show that the maximum static stress appears at the junction of blade and hub and is less than the yield strength of material, which is not enough to produce cracks. Based on one-way coupling technology, Zheng Jun [7] simulated the structure of centrifugal pump impeller under different working conditions, and obtained the changes of equivalent stress and maximum total deformation of centrifugal pump impeller. Based on the whole flow field of centrifugal pump, Huang Si [8] carried out one-way fluid-solid coupling analysis of rotor system, and the calculation results met the requirements of mechanical properties. For the stress analysis of liquid ring vacuum pump, Wang Hongjun [9] uses Ansys software to give a new rotor strength calculation method, which can accurately understand the size and position of stress and deformation

compared with the traditional calculation method.

Huang Haoqin [10] carried out uncoupled and bidirectional coupled unsteady numerical simulation of marine centrifugal pump, and carried out multi-phase analysis of rotor mode. The results show that the coupling mode has a certain influence on the impeller, stress and strain, and has little effect on the rotor mode. The maximum deformation and maximum equivalent stress of the two-way coupling are greater than those of the one-way fluid-solid coupling, and the transient phase is different. The rotor modal frequency and amplitude have certain pulsation. Liu Houlin [11] compared the residual heat removal pump rotor in the non-prestressed mode and the modal of the fluid-solid coupling force and the rotating centrifugal force. The results show that the influence of the fluid-solid coupling load force on the natural frequency of the rotor is greater than the rotating centrifugal force. Under the action of prestress, the amplitude increases.

At present, the mechanical analysis of impeller machinery has been relatively mature, but the mechanical research on the impeller of liquid ring pump mainly includes formula calculation and simple mechanical simulation. The structural analysis of impeller by fluid-solid coupling method is still lacking. In this paper, the one-way fluid-solid coupling analysis method is used to analyze the stress-strain and modal analysis of the liquid ring pump impeller, which has a certain reference effect on the structural design and optimization of the liquid ring pump impeller.

Flow field analysis of liquid ring pump

Geometric structure and internal flow field of liquid ring pump

The left and right sides of the double suction liquid ring vacuum pump are symmetrical. In order to reduce the amount of calculation, this paper adopts a unilateral structure, and the simplified structural model is shown in Fig.1(a). The impeller radius of the liquid ring pump is 390mm, the shell radius is 463mm, the number of blades is 19, the speed is 570r/min, and the inlet flow rate is 185m^3/min. Ignoring the axial clearance between the impeller end face and the suction and exhaust ports, the simplified model is mainly divided into the inlet and outlet extension section, the inlet extension section, and the area between the inner wall of the pump body and the impeller. The exhaust port is divided into a main exhaust port and 14 exhaust ports. The simplified model is meshed by FLUENT MESHING, and the polyhedral mesh is used. The number of meshes is 1 million. The simplified fluid domain mesh model of the liquid ring pump is shown in Fig.1(b).

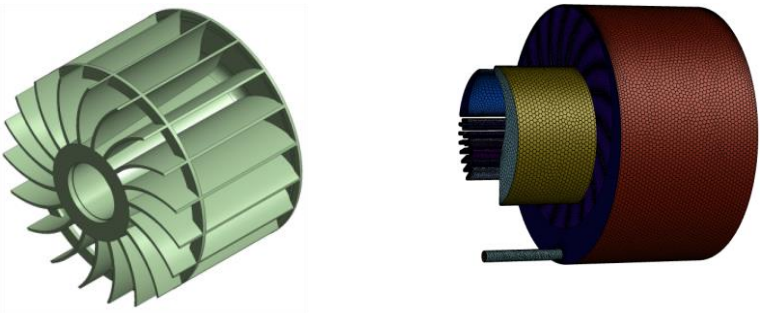

(a) Impeller geometry model *(b) Fluid domain grid*

Figure 1: Impeller structure and grid model

Numerical solution method

In order to study the unsteady characteristics of the internal flow field of the liquid ring pump, the VOF gas-liquid two-phase flow model is used to capture the gas-liquid interface of the liquid ring pump. The RNG k-ε turbulence model and PISO algorithm are used to couple the velocity field and pressure field. The surface of the shell and the blade adopts non-slip and adiabatic wall boundary conditions, and the influence of liquid surface tension is considered. The surface tension coefficient is 0.07. According to GB13929-2010 water ring vacuum pump and water ring compressor test method, set the suction medium (air) temperature is 20°C, the working water temperature is 15°C. Import adopts mass import, export adopts pressure export, and the pressure is 101325 Pa. The time step is 1×10^{-5}s. When the calculation time reaches 0.6s, the inlet pressure of the liquid ring pump tends to be stable. At this time, the numerical calculation tends to converge. In order to further ensure the accuracy of the data, the simulation results at 3 seconds are taken for detailed analysis.

Flow field calculation results

Figure 2 is the relative pressure cloud diagram of different axial sections of the liquid ring pump at *t*=3s. It can be seen from the diagram that the pressure gradually increases from the hub to the inner wall of the shell in the radial direction, and gradually increases from the suction zone to the compression zone in the circumferential direction. The maximum pressure of the inner wall of the shell in the exhaust zone and the minimum gas pressure at the beginning of the suction zone appear. The dotted line in Fig.2 is the gas-liquid interface, and it can be seen that there is a large pressure gradient near the gas-liquid interface. In the axial direction, the change of hub diameter has little effect on the pressure distribution, and the pressure distribution of each characteristic section is basically the same, but the area of low pressure area in the suction area increases gradually with the decrease of hub diameter.

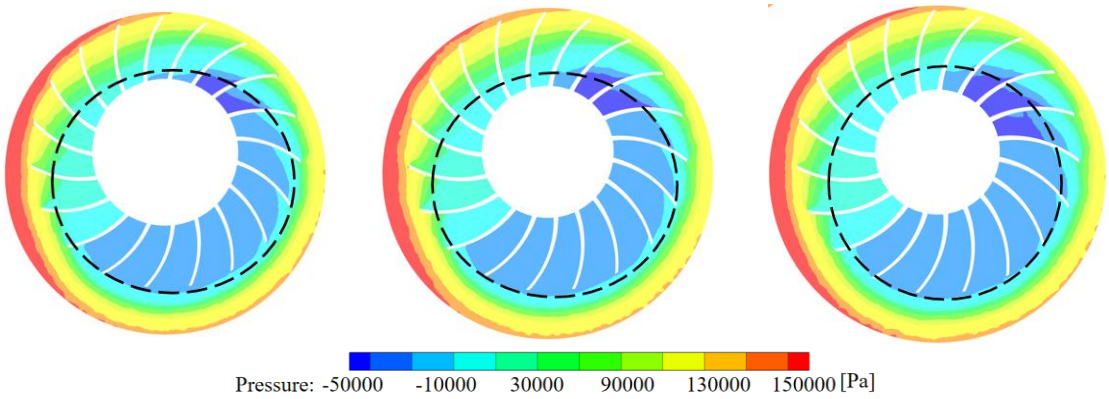

Figure 2: Cloud map of different cross-sectional pressures

In Mechanical, the fluid domain simulation pressure is imported into the impeller surface. The pressure applied to the impeller surface is shown in Fig.3. It can be seen from the figure that the pressure applied to the blade surface is different, and there is a pressure difference between the blade working surface and the pressure surface. It can be seen from Fig.2 that the pressure on the blade surface near the suction area is lower than that in the exhaust area. As the hub diameter increases, the pressure applied to the blade surface gradually increases.

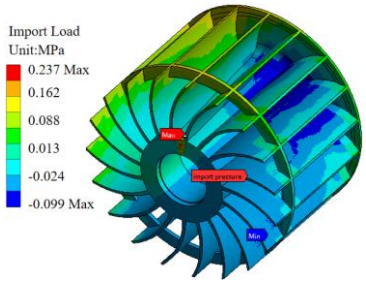

Figure 3: Load applied to blade surface

Structure analysis of impeller of liquid ring pump

Fluid-solid coupling calculation method

Fluid-solid coupling analysis mainly studies the interaction between flow field and solid model, which is mainly divided into two-way fluid-solid coupling and one-way fluid-solid coupling. Unidirectional fluid-solid coupling does not consider the influence of solid on the flow field. By calculating the internal flow field, the obtained fluid pressure is applied to the solid surface as a load for mechanical calculation. Because the deformation of the impeller of the liquid ring pump is very small compared with the size of the flow field, the influence of the solid deformation on the flow field is ignored, and the one-way fluid-solid coupling analysis method is adopted. The main analysis steps are: (1) flow field analysis; (2) Transfer the flow field results to only the structure field; (3) Coupling analysis and output results.

Structural parameters of liquid ring pump impeller

The main material of the liquid ring pump impeller is Q235B, and the material properties are set in Engineering Data. The main physical parameters are shown in Table 1.

Table 1: Physical parameters of impeller material

Material	Yield limit	Poisson ratio	Density	Allowable deformation
Q235B	235MPa	0.25	7.85g/cm^3	0.6mm

The impeller model of 2BEC42 liquid ring pump is established in Mechanical. The grid size is set to 6mm and the number of grids is 700,000. The grid model is shown in Figure 4(a) and Figure 4(b) shows the surface load and constraint diagram of the liquid ring pump impeller.

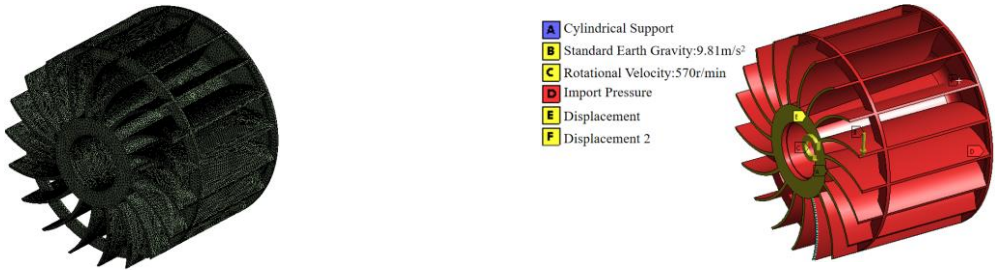

(a) Impeller grid *(b) Loads and constraints*

Figure 4: Impeller grid and its constraints

When the impeller works normally, the blade is in high-speed rotation and bears great centrifugal load. Therefore, when calculating the blade stress, the impeller rotation speed needs to be added. In addition, the cylindrical surface of the pump impeller shaft section is set as a cylindrical support, and the axial degree of freedom of the impeller is constrained. The radial and tangential directions are set to be free, and the fluid domain pressure is introduced to the surface of the pump impeller.

Analysis of total deformation and equivalent stress of impeller

Figure 5 shows the total deformation distribution of the pressure surface and suction surface of a single blade. It can be seen that the total deformation of the pressure surface of the blade is slightly larger than that of the suction surface. The deformation of the blade is mainly distributed near the outer edge of the blade. The deformation near the hub is small, and the deformation increases with the increase of the radius of the impeller. In addition, at the outer edge of the blade, the deformation gradually increases from the middle baffle to the end face of the impeller. However, due to the presence of stiffeners, the maximum deformation is located in the middle of the blade, and the maximum deformation is 0.12976mm, which is less than the allowable deformation of the material. The deformation near the stiffener is small, and the deformation increases gradually from the stiffener to the end face of the impeller.

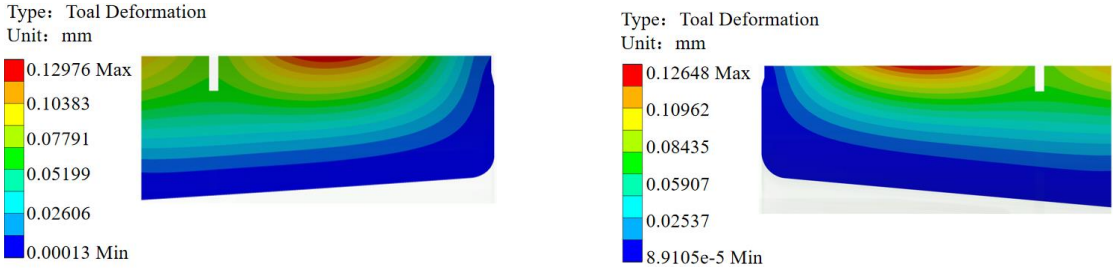

(a) Pressure face *(b) Suction surface*

Figure 5: Total deformation of single blade

Figure 6 shows the equivalent stress distribution of a single blade. It can be seen that the maximum stress of the blade pressure surface is higher than that of the blade suction surface. The maximum stress of the blade is located at the outer edge of the middle baffle of the impeller and the blade. The maximum equivalent stress is 20.221MPa, which is less than the yield strength of the material. In addition, the connection between the blade and the stiffener is also a place of stress concentration.

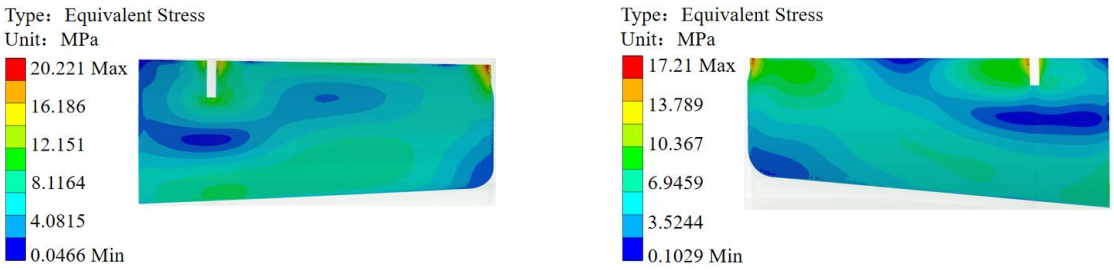

(a) Pressure face (b) Suction surface

Figure 6: Equivalent stress of single blade

Figure 7 shows the total deformation and equivalent stress distribution of the liquid ring pump impeller under various working conditions. It can be seen that the stress and deformation distribution under various working conditions are basically the same. Combined with the change curves of total deformation and equivalent stress with inlet flow in Fig.8, it can be seen that the total deformation of the impeller under each working condition is very small, and the maximum total deformation fluctuates within the range of 0.001mm. The maximum equivalent stress of the impeller decreases first and then increases with the increase of inlet flow, and the equivalent stress reaches the minimum at 180 m^3/min. In general, the maximum deformation of the impeller is 0.13 mm, less than the allowable deformation of 0.6mm, the maximum equivalent stress is 34.01MPa, less than the yield strength of 235MPa, and the mechanical performance parameters obtained by finite element calculation are within the allowable range, which meets the mechanical performance requirements.

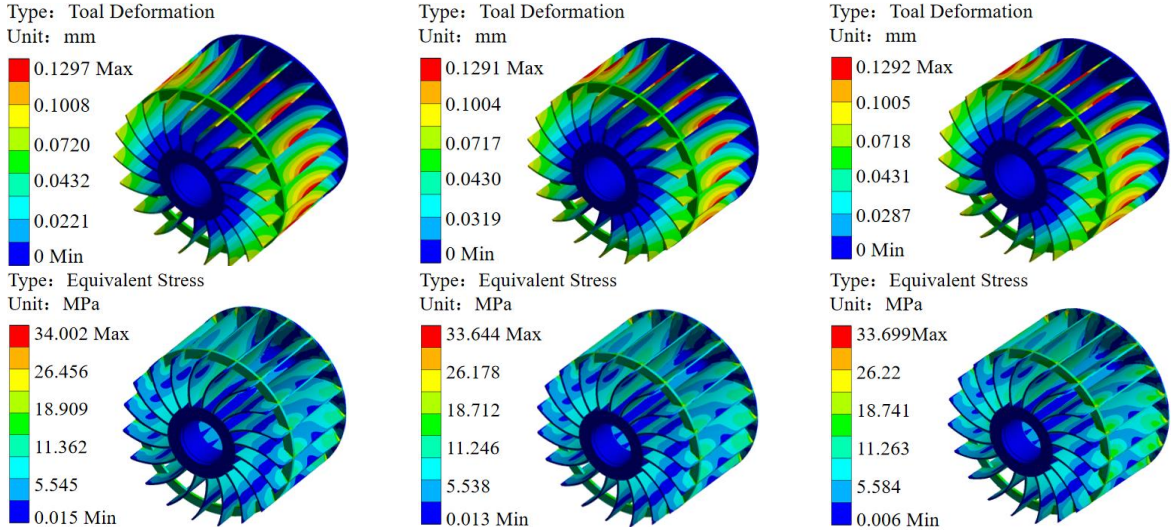

(a) 170m^3/min (b) 178m^3/min (c) 185m^3/min

Figure 7: Equivalent stress of impeller under different working conditions

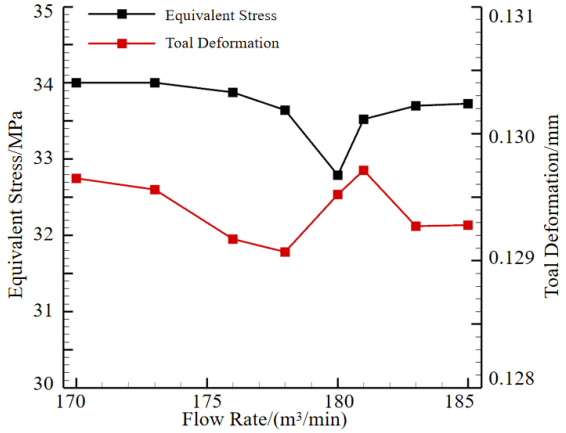

Figure 8: Curves of total deformation and equivalent stress of impeller changing with inlet flow rate

Impeller and shaft overall modal analysis

The modal analysis of the whole rotor system is carried out by using the modal module of ANSYS Workbench.Figure.9 is the first eight order frequency and vibration mode of the rotor system composed of liquid ring pump shaft and impeller.

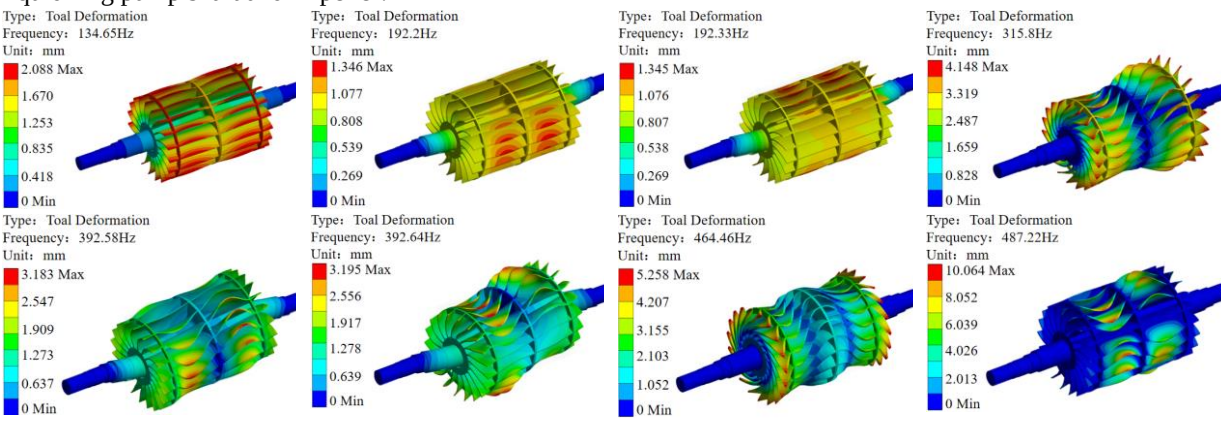

Figure 9: Modal of 1~8 order rotor system

It can be seen that the first-order vibration mode of the impeller is torsional vibration, and the deformation of the impeller gradually increases from the axis to the outer edge, which is approximately symmetrical along the middle baffle. The second and third order vibration modes are bending vibration, and the maximum deformation occurs in the middle of the impeller rim. The fourth-order vibration mode is torsional vibration, but compared with the first-order mode, the deformation of the fourth-order mode is mainly concentrated on the outer edge of the blade on both sides of the stiffener, and the deformation of the shaft and the middle diaphragm position is small. The fifth-order and sixth-order vibration modes are bending vibration. Compared with the second-order and third-order vibration modes, the deformation of the hub is small. The seventh-order vibration mode is torsional vibration, and the maximum deformation position is the outer edge of the end blade. The 8th order vibration mode is also bending vibration. The difference is that the deformation is mainly concentrated in the blade position of the diaphragm and the stiffener, and the deformation at other positions is small.

Table 2: The first 8 order natural frequency and maximum amplitude

Order	Frequency (Hz)	Maximum Amplitude (mm)	Order	Frequency (Hz)	Maximum Amplitude (mm)
1	134.65	2.088	5	392.48	3.183
2	192.2	1.346	6	392.64	3.195
3	192.33	1.345	7	464.46	5.258
4	315.81	4.148	8	487.22	10.064

Table 2 is the natural frequency and maximum amplitude of the first eight modes of the liquid ring pump. Combined with the 1 ~ 8 order vibration mode diagram, it can be seen that the maximum amplitude is higher when the impeller vibration mode is torsional vibration. The modal frequency of the impeller section is 134.65 Hz. According to the relationship between the speed and frequency, the first-order critical speed of the impeller is 8079 r / min by calculation. Under normal operation, the impeller speed is much lower than the first-order critical speed, and resonance will not occur.

Conclusion

The maximum total deformation of the liquid ring pump impeller is located at the outer edge of the impeller, and the maximum stress is located at the connection between the blade and the distribution plate. The stress and deformation distribution under each working condition are basically the same. The maximum equivalent stress decreases first and then increases with the inlet flow rate. The maximum deformation is 0.13mm, and the maximum equivalent stress is 34.01MPa, which meets the material performance requirements.

The total deformation and maximum stress of the blade pressure surface are higher than those of the suction surface. From the middle baffle to the impeller section, the deformation of the outer edge of the blade gradually

increases. The stiffener effectively alleviates the deformation of the impeller edge and reduces the deformation of the outer edge of the impeller end face.

When the vibration mode of the impeller is torsional vibration, the maximum amplitude is high, the impeller speed is far less than the first-order critical speed, and resonance phenomenon will not occur.

Reference

[1]. Gao Fang. Theoretical and simulation research on structural parameters of liquid ring pump [D]. Northeast Petroleum University, 2006.

[2]. Matteo Pellegri, Venkata Harish Babu Manne, Andrea Vacca. A simulation model of Gerotor pumps considering fluid–structure interaction effects: Formulation and validation [J]. Mechanical Systems and Signal Processing, 140(2020) 106720.

[3]. Mahendhar Kumar, Akash Venkateshwaran, Machavolu Sai Santhosh Pavan Kumar, et al. Strength analysis of a regenerative flow compressor and a pump based on fluid-structure coupling [J]. Materials Today: Proceedings, 51(2022) 1619-1624

[4]. Li Peijian, Cao Yongle, Yue Guosen, et al. Fluid-structure Interaction Analysis of High Speed Tangential Pump Impeller [J]. Missiles and Space Vehicles, 2022(03):22-26+36.

[5]. Zhang Xin, Zheng Yuan, Mao Xiuli, et al. Strength analysis of axial flow pump impeller based on fluid-solid coupling [J]. Water Resources and Power, 2014, 32(07):137-139+150.

[6]. Zhang Xin, Zheng Yuan, Qian Jun, et al. Modal analysis of horizontal axial flow pump impeller based on fluid-solid coupling [J]. 2015, 33(07): 164-167.

[7]. Zhu Li, Yang Changming, Zheng Jun, et al. Structure Analysis of Axial Flow Pump Impeller Based on Fluid-solid Coupling [J]. Fluid Machinery, 2013, 41(03): 20-23+40.

[8]. Zheng Jun, Yang Changming, Zhu Li, et al. Fluid-structure Coupling Analysis of Centrifugal Impeller [J]. Fluid Machinery, 2013, 41(02): 25-29.

[9]. Huang Si, Zhang Xuejiao, Su Xainghui, et al. Fluid-solid Interaction Analysis of Centrifugal Pump Based on Whole Flow Field [J]. Fluid Machinery, 2015, 43(11): 38-42.

[10]. Wang Hongjun, Huang Si, Guan Jun, et al. Numerical analysis of mechanical properties of rotor in liquid-ring vacuum pump [J]. Vacuum, 2010, 47(01): 15-18.

[11]. Liu Houlin, Xu Huan, Wang Kai, et al. Modal Analysis for Rotor of Residual Heat Removal Pump based on Fluid-structure Interaction[J]. Fluid Machinery, 2012, 40(06): 28-32.